JOURNAL OF VIROLOGY, Apr. 2006, p. 3592–3606 Vol. 80, No. 7
0022-538X/06/$08.00+0 doi:10.1128/JVI.80.7.3592–3606.2006

Herpes Simplex Virus Type 1 Accumulation, Envelopment, and Exit in Growth Cones and Varicosities in Mid-Distal Regions of Axons

Monica Miranda Saksena,[1] Hiroyuki Wakisaka,[1]† Bibing Tijono,[1] Ross A. Boadle,[2] Frazer Rixon,[3] Hirotaka Takahashi,[1]† and Anthony L. Cunningham[1]*

Centre for Virus Research, Westmead Millennium Institute, Westmead Hospital, P.O. Box 412, Westmead, NSW 2145, and The University of Sydney, Sydney, Australia[1]; Electron Microscope Laboratory, ICPMR, Westmead Hospital, Westmead, NSW 2145, Australia[2]; and MRC Virology unit, Institute of Virology, Church Street, Glasgow G11 5JR, United Kingdom[3]

Received 1 September 2005/Accepted 9 January 2006

The mechanism of anterograde transport of alphaherpesviruses in axons remains controversial. This study examined the transport, assembly, and egress of herpes simplex virus type 1 (HSV-1) in mid- and distal axons of infected explanted human fetal dorsal root ganglia using confocal microscopy and transmission electron microscopy (TEM) at 19, 24, and 48 h postinfection (p.i.). Confocal-microscopy studies showed that although capsid (VP5) and tegument (UL37) proteins were not uniformly present in axons until 24 h p.i., they colocalized with envelope (gG) proteins in axonal varicosities and in growth cones at 24 and 48 h p.i. TEM of longitudinal sections of axons in situ showed enveloped and unenveloped capsids in the axonal varicosities and growth cones, whereas in the midregion of the axons, predominantly unenveloped capsids were observed. Partially enveloped capsids, apparently budding into vesicles, were observed in axonal varicosities and growth cones, but not during viral attachment and entry into axons. Tegument proteins (VP22) were found associated with vesicles in growth cones, either alone or together with envelope (gD) proteins, by transmission immunoelectron microscopy. Extracellular virions were observed adjacent to axonal varicosities and growth cones, with some virions observed in crescent-shaped invaginations of the axonal plasma membrane, suggesting exit at these sites. These findings suggest that varicosities and growth cones are probable sites of HSV-1 envelopment of at least a proportion of virions in the mid- to distal axon. Envelopment probably occurs by budding of capsids into vesicles with associated tegument and envelope proteins. Virions appear to exit from these sites by exocytosis.

In humans, herpes simplex virus type 1 (HSV-1) enters via the mucosa or breaks in the skin. After replication in the epithelial cells, the virions infect the nerve endings of dorsal root ganglion (DRG) neurons innervating the infected tissue. The virus is then transported via retrograde axonal transport to the neuronal-cell body, where a lifelong latent infection is established. Reactivation of HSV-1 from latency results in anterograde axonal transport of the virus from the cell body to the nerve terminals to reinfect cells in the skin or mucosa. Reactivation of HSV-1 during a patient's lifetime is frequent, resulting in either recurrent symptomatic disease or asymptomatic virus shedding (45, 52).

For many years, there has been controversy about the mechanism of assembly and egress of alphaherpesviruses in cultured cell lines. Until recently, there were two opposing models to explain the events following capsid assembly in the nucleus and subsequent budding through the inner nuclear membrane. The first model proposes that there is direct transport of enveloped capsids within vesicles from the outer nuclear membrane via the trans-Golgi network to the plasma membrane, where they are released by exocytosis (8, 24). The second model proposes that enveloped capsids undergo de-envelopment at the outer nuclear membrane and secondary reenvelopment at the trans-Golgi network. The enveloped capsids are then transported within a vesicle to the plasma membrane and then released by exocytosis. Only recently has sufficient evidence accumulated in favor of the second model (33, 34, 47, 49, 51). However, in neurons there is an added level of complexity, with virus egress occurring from both the cell body of the neurons and the distal axon terminus in vivo.

The process of alphaherpesvirus assembly and egress in the cell body of DRG neurons appears to be similar to that in cultured cell lines (15, 20, 33, 34, 35, 36, 47). However, recent findings have increased the controversy regarding the mechanism of anterograde transport and assembly in axons (10). The findings of either enveloped capsids or unenveloped capsids or both within axons by different investigators have suggested two hypotheses. Early observations of enveloped capsids in vesicles within neuronal processes, probably axons, suggested that fully assembled virions in vesicles in the cell body are transported into the axon and then to the axon terminus, where virions are released by exocytosis (3, 30, 31). However, in these reports, whether in neurons of the peripheral or central nervous system of rabbit or rodent models in vivo or in vitro, the region of the axon in which these enveloped capsids were observed was either proximal (close to the cell body) or uncertain. In addition, either single or a few enveloped virions were demonstrated in axons (Table 1). In several studies, both enveloped and unenveloped capsids were observed in axons (21, 22, 25, 26, 43). Furthermore, clusters of enveloped capsids were often

* Corresponding author. Mailing address: Centre for Virus Research, Westmead Millennium Institute, P.O. Box 412, Westmead, NSW 2145, Australia. Phone: 61298459001. Fax: 61298459100. E-mail: tony_cunningham@wmi.usyd.edu.au.

† Present address: Department of Otolaryngology, Ehime University, Shizkawa, Toon-City, Ehime, Japan 791-0295.

TABLE 1. Identification of alphaherpesvirus virions in axons by TEM or TIEM

System[a]	Site of viral particles in axon	Observations[b]	Reference
Enveloped virions			
HSV—chick embryo DRG	Uncertain	No virions in axons	22
HSV—rabbit optic nerve (retinal ganglia)	Uncertain	Enveloped virions in cisternae (ER); occasional unenveloped capsids	25
HSV—mouse DRG	Proximal	Single enveloped virion; no MTs visible	7
HSV—mouse DRG, celiac ganglion	Proximal uncertain	Periaxonal virions; atypical particles in vesicle-rich region	53
HSV—dissociated rat DRG; in vitro	"Neuritic extension"	Three enveloped virions; no MTs visible	30
PRV—rat CNS sensory vagal processes	Uncertain	Single enveloped virions; no MTs visible	3
HSV—mouse trigeminal ganglion	? Proximal	Several enveloped virions; no MTs visible	26
PRV—sympathetic ganglia	Proximal (and axon hillock)	Many enveloped virions	5, 10
PRV—sympathetic ganglia	Midaxon	Two enveloped virions	5
Unenveloped virions			
HSV—DRG, two-chamber system	Mid-distal	Capsids surrounded by MTs	44
HSV—DRG two-chamber system	Mid-distal	Capsids surrounded by MTs; VP5-VP16 colocalization on particles, but not with gB by TIEM	23
HSV—dissociated rat DRG; in vitro	Uncertain	VP5-labeled capsid in axon by TIEM	35
HSV—dissociated DRG	Uncertain	Capsid labeled for VP16 in axon	36
HSV—mouse trigeminal ganglion	Midaxon	U/E capsids identified by TIEM and adjacent to MTs	43
PRV—sympathetic ganglia	Proximal	Two U/E capsids after BFA inhibition	10
HSV—mouse retinal ganglia	Midaxon	Unenveloped capsids (VP5 immunolabeled) (?) enveloped virions	27
Both enveloped and unenveloped virions			
HSV—suckling mice, spinal cord	Uncertain	Single U/E capsid in unmyelinated axon; cluster of enveloped virions in cisternae (ER) (myelinated axon)	21
PRV—mouse DRG	Proximal	Several enveloped virions in vesicle-rich region	16
PRV—sciatic nerve	Midaxon	Enveloped and unenveloped virions (not shown)	
HSV—DRG in vitro	Mid-distal axon, growth cones, varicosities	Enveloped and U/E capsids in varicosities and growth cones (and adjacent axon)	This study

[a] CNS, central nervous system.
[b] U/E, unenveloped; MT, microtubule; ER, endoplasmic reticulum; BFA, brefeldin A.

demonstrated in cisternae, thought to be part of the agranular endoplasmic reticulum, or in vesicle-rich regions (21, 25).

An alternative mechanism was suggested by observations of unenveloped HSV-1 capsids in direct apposition to microtubules during anterograde axonal transport in the distal regions of axons interacting with autologous human epidermal explants in the external chamber of a two-chamber system (44). Follow-up observations of infected axons in this system by transmission immunoelectron microscopy (TIEM) showed unenveloped capsids, adjacent to microtubules, immunolabeled for capsid VP5 and surrounded by tegument proteins (VP16), whereas glycoproteins and other tegument proteins were observed within axonal vesicles in distal axons (23, 36). Unenveloped capsids were demonstrated in infected axons during anterograde transport, but not in uninfected axons, by controlled and blinded electron microscopy observations and by both TIEM and scanning immunoelectron microscopy. In our laboratory, previous studies have observed more than 100 unenveloped particles, but no enveloped capsids, in the mid- or distal axon, usually in cross sections (references 23, 35, 36, and 44 and unpublished observations). These studies were further supported by the examination of capsid, tegument, and envelope protein localization by serial fixation and immunofluorescence assay, demonstrating differences in the kinetics of glycoprotein and capsid protein appearance in axons and the inhibition of transport of glycoproteins, but not capsid proteins, with brefeldin A. Furthermore, intact unenveloped capsids were detected in axons by transmission electron microscopy (TEM) in neurons treated with brefeldin A (35), and the tegument protein US11 was found to directly interact with the heavy chain of the anterograde molecular motor kinesin (11). The above observations suggested separate capsid and glycoprotein transport and assembly at the axon terminus (although the latter has not been visualized). Other laboratories have also provided further evidence for such anterograde axonal transport of unenveloped HSV-1 capsids (27, 42, 43).

However, two recent reports from the same laboratory challenged this "separate transport" or "subassembly" hypothesis (5, 10). Del Rio et al., using dual red-fluorescent-protein-/green-fluorescent-protein (GFP)-labeled pseudorabies virus (PRV) in cultured rat superior cervical ganglion (SCG) neurons showed a heterogeneity in GFP-labeled VP22 fluorescence that was similar in purified virions, the cell body, and axons of neurons. They also showed large numbers of enveloped particles in the proximal axon. The transport of these enveloped capsids was inhibited by brefeldin A, leaving a small number of unenveloped capsids within the proximal axon (10). In a three-chamber system, enveloped particles within vesicles were also observed within the midaxon (5).

Therefore, the literature now contains two sets of observations, one in which investigators have observed enveloped HSV-1 capsids within proximal axons and PRV in proximal and midaxons, while in the other, we and others have observed unenveloped capsids in cross sections of mid- and distal regions of axons, clearly defined by the two-chamber system (Table 1).

In this study, we add a further dimension to the understanding of viral anterograde transport, using serial fixation and colocalization of all three classes of viral proteins, capsid, tegument, and glycoprotein, in human fetal DRG axons. Application of in situ fixation and longitudinal sectioning of DRG cultures has enabled the identification and visualization of the entire mid- and distal regions of axons and their specialized regions, growth cones and varicosities. We demonstrate colocalization of viral capsid, tegument, and envelope proteins and accumulation of enveloped and unenveloped capsids in specific regions of the mid- and distal axon, namely, the varicosities and growth cones. Free envelope and tegument proteins in apposition to axonal vesicles within the growth cones were observed by TIEM. Furthermore, we show partially enveloped capsids within these varicosities and growth cones, suggesting that virions can assemble at these sites.

MATERIALS AND METHODS

Cells and viruses. Virus stocks were passaged in HEp-2 cells as previously described (35, 36). A clinical isolate of HSV-1 (CW1) was used in both confocal and electron microscopy studies. vUL37-GFP virus was used in confocal-microscopy studies.

Construction of vUL37-GFP virus. HSV-1 strain 17 DNA has a single SpeI restriction enzyme site at the 3′ end of the UL37 open reading frame. To generate the UL37-GFP fusion, an in-frame SpeI site was engineered at the N terminus of the GFP open reading frame in the expression vector pGFPemd-b″ (Packard Bioscience). A second SpeI site was introduced into the SalI site downstream from the GFP stop codon in pGFPemd-b to generate the plasmid pGFPSpe2. The purified GFP fragment from SpeI-digested pGFPSpe2 was ligated with SpeI-digested HSV-1 strain 17 virion DNA. The ligated DNA was transfected into BHK cells using Lipofectin (Invitrogen). After 4 days, the culture medium was harvested and titrated on BHK cells. Green-fluorescing plaques were purified through three cycles of plaque picking. One isolate (designated vUL37-GFP) was selected and grown to high titer on Hep2 cells. The presence of the UL37-GFP fusion protein was confirmed by Western blotting of infected cells and purified virions (data not shown).

The kinetics of vUL37-GFP and parental strain 17 growth in BHK cells were similar over 30 h as measured by single-step growth curves (data not shown). vUL37-GFP infected and replicated in neurons with kinetics similar to those of the clinical strain CW1 (data not shown).

Single-step growth curve for vUL37-GFP virus. BHK-21 clone 13 cells were cultured in Glasgow in minimal essential medium supplemented with 10% tryptose phosphate broth and 10% newborn calf serum (ETC10). Replicate 35-mm plates were infected with 5 PFU/cell of HSV-1 strain 17 or vUL37-GFP. A sample of each virus inoculum was retained as the zero-hour time point. After 1 h at 37°C, the virus inoculum was removed. The cells were washed and overlaid with 2 ml of fresh ETC10 and replaced at 37°C. Individual plates were harvested at 1 (immediately after the addition of fresh overlay medium), 3, 6, 9, 12, 18, 24, and 30 h p.i. and stored at −70°C. Samples were sonicated, and virus titers were estimated by titration on BHK cells (data not shown).

Antibodies. Antibodies as specified were kindly provided by the following investigators: rabbit antibody against VP5 from Gary Cohen and Roselyn Eisenberg, University of Pennsylvania, Philadelphia, PA (6); rabbit antibody against VP22 from Peter O'Hare, Marie Curie Institute, Oxted, United Kingdom (14); mouse antibody against gG from Tony Minson, University of Cambridge, United Kingdom (32); and guinea pig antibody against gD from David Bernstein, Cincinnati Children's Hospital Medical Centre and the University of Cincinnati, Cincinnati, Ohio. Fluorescein isothiocyanate-conjugated antibodies were purchased from Sigma. Fluorolink Cy5- and Cy3-conjugated antibodies were purchased from Amersham Life Science. Gold-conjugated antibodies were obtained from British Biocell International.

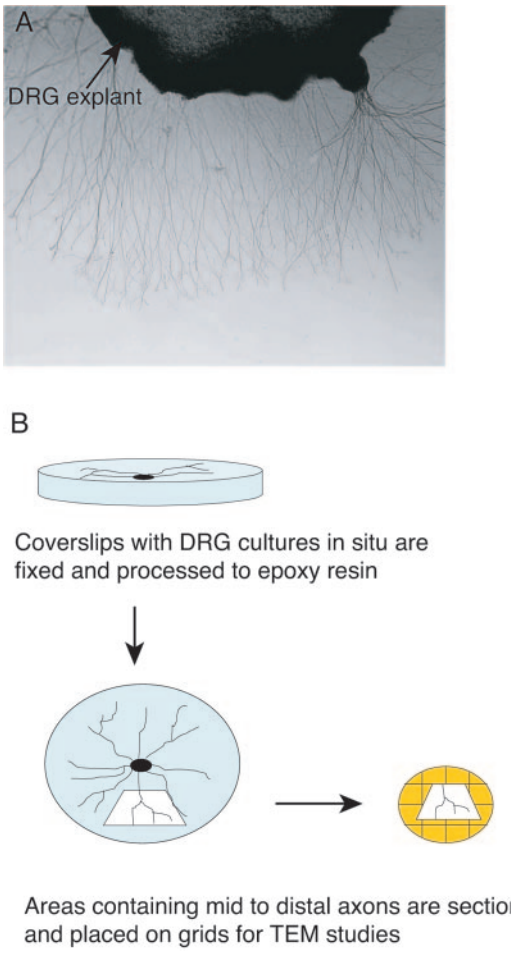

FIG. 1. Overview of the human fetal DRG cultures on coverslips and processing for TEM. (A) Photomicrograph of the explanted DRG with axons extending randomly from the ganglia. (B) Schematic diagram showing the fixation and processing of DRG cultures in situ and the precise selection of the mid- and distal regions of axons for longitudinal sections and TEM examination.

Preparation of human fetal DRG explants. DRG were prepared from human fetal tissue obtained at therapeutic termination with the informed consent of the mother. Protocols were approved by the Research Ethics Committee of the Western Sydney Area Health Service (now known as the Sydney West Area Health Service). The DRG were dissected, cleansed of connective tissue, placed onto Matrigel coated-glass coverslips, and cultured for 5 to 7 days to allow axon outgrowth (Fig. 1).

HSV-1 infection of DRG cultures. For confocal and electron microscopy studies of anterograde transport of HSV-1, DRG cultures were infected either with CW1 (10^5 PFU/0.5 ml/ganglion) or with vUL37 GFP virus (5×10^5 PFU/0.5 ml/ganglion). After 2 h, the inoculum was removed. The cultures were washed twice, and fresh medium was added. The infected cultures were incubated at 37°C under 5% CO_2 for 17, 22, or 46 h. The cultures were washed three times in phosphate-buffered saline and processed for either confocal microscopy or electron microscopy. For studies of HSV-1 entry into axons, DRG cultures were infected with the clinical isolate CW1 (10^5 PFU/0.5 ml/ganglion). The inoculum was removed at 1 or 1.5 h p.i., and the cultures were washed three times prior to fixation for electron microscopy. Mock-infected cultures were incubated in medium and fixed at 1, 1.5, 19, 24, or 48 h p.i.

Detection of infectious HSV-1 particles in the supernatants of DRG cultures. Cultures of human fetal DRG were infected with clinical isolate CW1 (10^5 PFU/0.5 ml/ganglion). After 2 h, the inoculum was aspirated. The cultures were washed twice, and fresh medium was added. Samples of supernatant were taken at 3, 6, 24, and 48 h p.i. for virus quantification on human fibroblasts. Virus quantification was performed by a fluorescent-focus assay using an antibody to

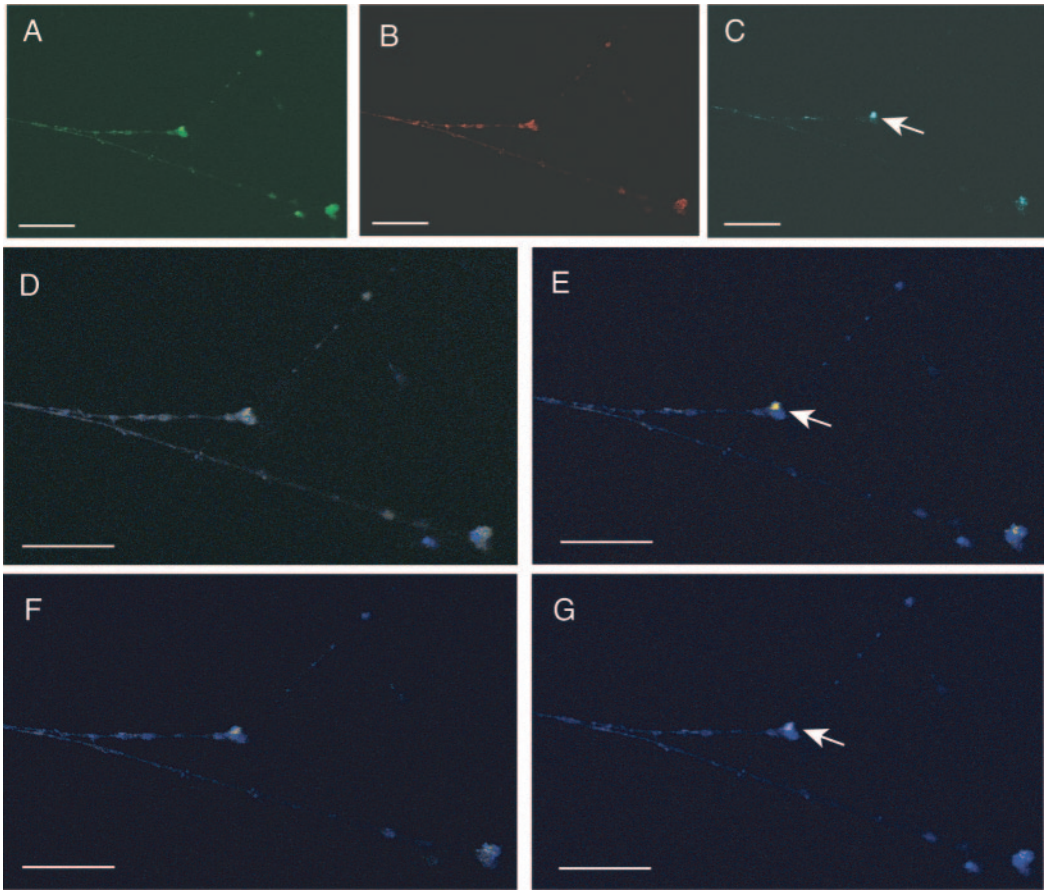

FIG. 2. Distribution and colocalization of VP5, gG, and UL37 proteins in distal axons and growth cones of HSV-1-infected human DRG at 24 h p.i. Human DRG explants were grown on Matrigel-coated coverslips and infected with vUL37-GFP virus. After 24 h p.i., the cultures were fixed, permeabilized, and labeled simultaneously with antibodies to capsid VP5 and envelope glycoprotein gG. VP5, UL37, and gG antigens were distributed throughout the axon with concentrations of fluorescence at varicosities and growth cones (A, B, C). Foci of colocalization between two or three antigens were found at the varicosities and growth cones (arrows) (D to G). The images show UL37-GFP as green (A), VP5 as red (B), and gG as cyan (C). Overlay images of dual colocalization in yellow and free (not colocalized) antigens in blue are shown for VP5 and UL37 (D), for UL37 and gG (E), and for VP5 and gG (F). Triple colocalization (white) and noncolocalized antigens (blue) are shown in panel G. Bars, 40 μm.

HSV-1 gC (Syva Microtrak). This experiment was conducted twice with replicate cultures, and the results were expressed as mean titers.

Immunofluorescence and confocal microscopy. DRG cultures were processed for immunofluorescence and confocal microscopy as previously described (35). Colocalization between two or more fluorochromes was determined using the dyadic Boolean calculation process from the Leica TCS SPII confocal software (Leica Microsystems Heidelberg, Germany). Image analysis using the Boolean "AND" operator was performed to visualize colocalization between antigens. The Boolean "XOR" operator was used to visualize areas showing no colocalization between antigens.

TEM. Coverslips with DRG cultures in situ were fixed in modified Karnovsky's fixative (2.5% formaldehyde [freshly prepared from paraformaldehyde], 2.5% glutaraldehyde in 0.1 M MOPS [morpholinepropane sulfonic acid] buffer, pH 7.4). The cultures were fixed for 1 h at room temperature and then processed with Spurr epoxy resin as previously described (35, 36). Following polymerization, the coverslips were separated from the resin by plunging them into liquid nitrogen, leaving the DRG explant and axons exposed on the surface of the block. Areas in the blocks containing mid- to distal regions of axons were selected. Ultrathin sections (70 nm) were collected and examined using a Philips CM120 BioTWIN transmission electron microscope at 100 kV (Fig. 1).

For anterograde transport of HSV-1, 1,206 axon processes were examined at 24 h p.i. and 768 at 48 h p.i. To investigate entering virus at early time points, 409 axon processes were examined.

Statistics. Data were analyzed using the statistical software package SPSS for Windows version 12. Fisher's exact test was used to test for association between the distribution of unenveloped or enveloped capsids and sites within axons (growth cones, varicosities, or intervening regions of axons). The Pearson chi-square test was used to test for association between the numbers of extracellular capsids and time. A 5% level of significance was assumed throughout.

TIEM. DRG cultures were processed by freeze substitution as previously described (35, 36).

Immunolabeling. Tissue sections were dual immunolabeled using primary antibodies against tegument protein VP22 and envelope glycoprotein D and secondary antibodies conjugated to 5- and 10-nm gold particles as previously described (36).

RESULTS

In this study, confocal microscopy and electron microscopy were used to examine the assembly and egress of two strains of HSV-1 in axons of cultured human fetal DRG explants. DRG axons were approximately 4 to 5 mm in length, branched frequently, and had numerous axonal swellings, or varicosities, along their lengths. The varicosities could be seen by confocal microscopy as irregular-shaped swellings between two and eight times the diameter of the axon and were usually located at branch points, as previously described (1, 2, 39, 50, 54). The cultures were then fixed at 24 and 48 h p.i. and processed in situ for confocal microscopy and electron microscopy. For

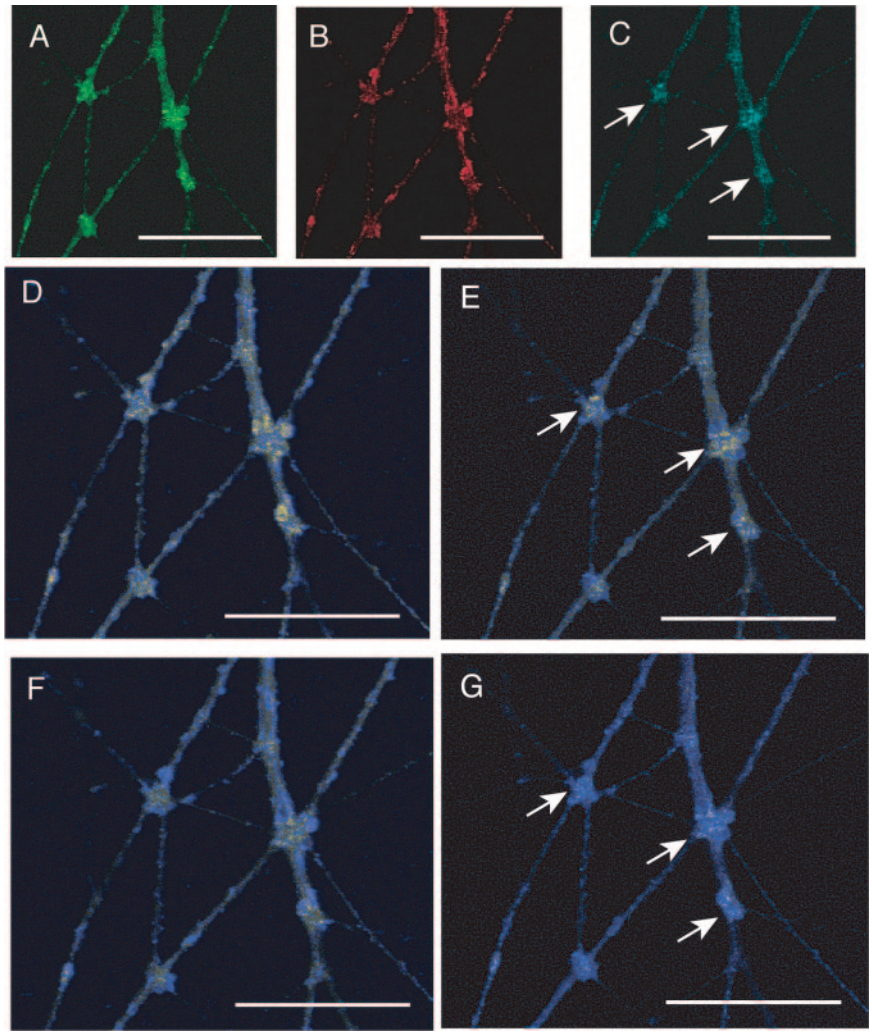

FIG. 3. VP5, gG, and UL37 proteins colocalized in axonal varicosities in midregions of axons of HSV-1-infected human DRG at 48 h p.i. Cultures of DRG explants were infected with vUL37-GFP virus, fixed, permeabilized, and labeled simultaneously with antibodies to VP5 and gG. All three antigens were distributed throughout the axon, with concentrations of fluorescence present at varicosities (arrows) (A, B, C). Foci of colocalization of two or three antigens were found at the varicosities (arrows). The images show UL37-GFP as green (A), VP5 as red (B), and gG as cyan (C). Overlay images of dual colocalization in yellow and free (not colocalized) antigen in blue are shown for VP5/UL37 (D), for UL37/gG (E), and for VP5/gG (F). Triple colocalization (white) and free antigen (blue) are shown in panel G. Bars, 40 μm.

TEM studies, we examined longitudinal sections of the mid- and distal regions of axons in situ, and this was critical for the identification of varicosities and growth cones. Varicosities with the ultrastructural appearance of growth cones were located in the vicinity of axonal branches and appeared to be formed by the growth of the axon termini beyond the expanded vesicle-rich region of the growth cone, consistent with published observations (1, 2, 19, 50, 54). The ultrastructural appearances of varicosities and growth cones were similar in infected and uninfected neurons.

HSV-1 capsid protein VP5, tegument protein UL37, and envelope glycoprotein gG colocalize in axonal varicosities and growth cones. After infection of DRG cultures with the HSV-1 clinical isolate CW1 or with vUL37-GFP, the distribution of capsid protein VP5, tegument protein UL37 (vUL37-GFP only), and envelope glycoprotein gG were examined by confocal microscopy at 19, 24, and 48 h p.i. Although UL37 and VP5 were not consistently present in axons at 19 h p.i., by 24 and 48 h p.i., labeling for VP5, UL37, and gG was distributed throughout the axon, with concentrations of antigen present at varicosities, often located at axonal branch points, and at growth cones (Fig. 2, 3, and 4). Colocalization between two or more fluorochromes was determined using the dyadic Boolean calculation process from the Leica confocal software. Image analysis using the Boolean "AND" operator was performed to visualize colocalization between antigens. The Boolean "XOR" operator was used to visualize areas showing no colocalization between antigens. Colocalization of all three antigens, VP5, UL37, and gG (triple colocalization), was mostly detected in intense foci in varicosities and growth cones (Fig. 2, 3, and 4) whereas free (not colocalized) antigen was diffusely distributed throughout the axons, varicosities, and growth cones

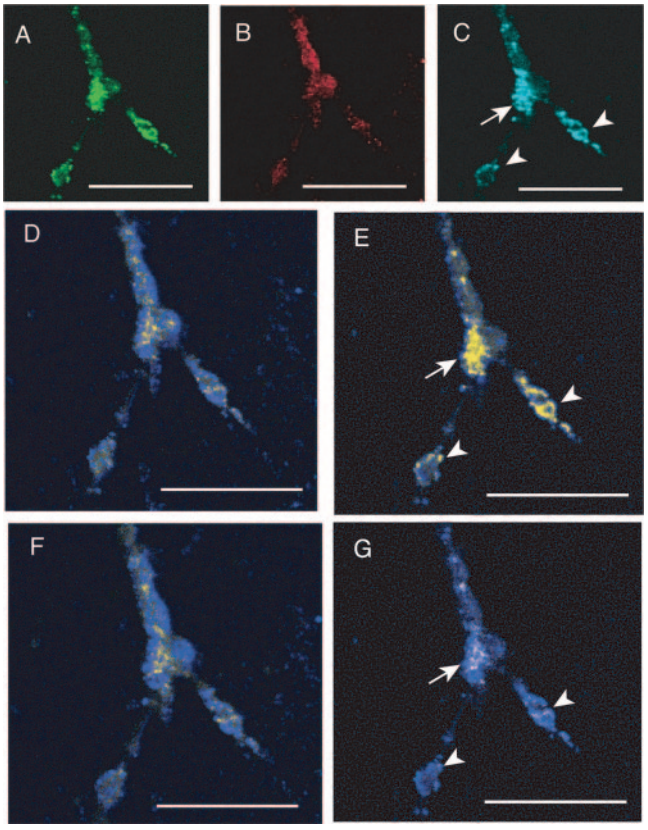

FIG. 4. VP5, gG, and UL37 proteins colocalized in axonal varicosities and growth cones in distal regions of axons of HSV-1-infected human DRG at 48 h p.i. Cultures of DRG explants were infected with vUL37-GFP virus, fixed, permeabilized, and labeled simultaneously with antibodies to VP5 and gG. All three antigens were present in intense foci in varicosities (arrows) and growth cones (arrowheads) (A, B, C). Foci of colocalization of two or three antigens were found in varicosities (arrows) and growth cones (arrowheads). The images show UL37-GFP as green (A), VP5 as red (B), and gG as cyan (C). Overlay images of dual colocalization in yellow and free (not colocalized) antigens in blue are shown for VP5/UL37 (D), for UL37/gG (E), and for VP5/gG (F). Triple colocalization (white) and free antigen (blue) are shown in panel G. Bars, 40 μm.

(Fig. 2, 3, and 4). At 48 h p.i., there was a marked increase in the intensity of fluorescence compared to 24 h p.i. (data not shown). Colocalization of all three antigens in the mid- and distal regions of axons (compared to 24 h p.i.) (data not shown) was mostly in the varicosities and growth cones. Analysis of the dual colocalization between VP5/UL37, VP5/gG, and UL37/gG showed a distribution similar to that of the triple colocalization. However, the precise locations of the foci of colocalization within the varicosities and growth cones differed between combinations of VP5/UL37, VP5/gG, and UL37/gG. For each pairwise combination, analysis of the distribution of free versus colocalized antigens was examined. In all colocalization studies, more free than colocalized antigen was found diffusely distributed throughout the axons, including varicosities and growth cones (Fig. 2, 3, and 4).

Enveloped, partially enveloped, and unenveloped capsids were present in axonal varicosities and growth cones. Using TEM, axonal varicosities and growth cones were identified in control or infected axons by their distinctive morphologies. The varicosities showed a disruption in microtubules, so they had fewer microtubule bundles. They also contained numerous vesicles of various sizes, resembling growth cones ultrastructurally. The growth cones were readily visible among the distal axonal processes and showed the typical ultrastructural morphology. This consists of a central region containing a high concentration of heterogeneous vesicles (clear and dense core vesicles), mitochondria, and a few microtubules, which are continuous with the axon that precedes the growth cone, and a peripheral domain rich in actin filaments (Fig. 5) (1, 2, 9, 19, 38, 39, 50, 54).

Unenveloped HSV-1 capsids were seen in mid- and distal regions of axons in varicosities and growth cones and in regions of axons between varicosities and growth cones, where they were in direct apposition to microtubules (Fig. 6A and 7A and D and Table 2; also see Fig. 9A). The unenveloped capsids had a distinctive morphology similar to that previously reported only in axons of HSV-infected neurons (23, 35, 36) and were not present in uninfected cultures in this study (Fig. 5). Enveloped capsids were also observed in vesicles in varicosities and growth cones and, rarely, in regions of the axons immediately adjacent to varicosities and growth cones (Fig. 6C and 7A, C, and D and Table 2; also see Fig. 9A). Clusters of unenveloped and enveloped capsids were observed, but only in varicosities or growth cones (Fig. 7D). Unenveloped and enveloped capsids can be directly compared in such clusters. In addition, partially enveloped capsids were identified in both varicosities and growth cones, mostly at 24 h p.i. (Fig. 6B and 7B and Table 2). These capsids were partially surrounded by an electron-dense vesicular membrane, consistent with invagination of the vesicle. (Fig. 6B and 7B) and were similar to those observed surrounding enveloping capsids in the cytoplasm of infected cell lines or in the cell bodies of neurons (20, 34, 36).

To determine whether such partially enveloped capsids might be due to endocytosis of virions by axons, human DRG cultures were infected and examined by TEM at 1 and 1.5 h p.i., guided by previous kinetic studies (13, 30, 35). Enveloped capsids adherent to the plasma membranes of axons, as well as submembranous unenveloped capsids, were readily observed. No enveloped capsids within vesicles or partially enveloped capsids were observed (Fig. 8).

The numbers of viral particles in the mid- and distal regions of axons were determined by examining 1,206 axon processes at 24 h p.i. and 768 at 48 h p.i. (Table 2). There was a statistically significant difference between the distributions of enveloped and unenveloped particles by site (Fisher's exact test, $P < 0.001$). The proportions of enveloped capsids in vesicles detected in varicosities and growth cones at 24 and 48 h p.i. were consistently higher than the numbers of unenveloped capsids in each of these sites, (i.e., varicosities, 20.8% unenveloped capsids at 24 and 48 h [95% confidence interval {CI}, 9.3%, 32.3%]; growth cones, 19.1% unenveloped capsids at 24 and 48 h [95% CI, 7.9%, 30.4%]), whereas the proportion of unenveloped capsids in the intervening regions of axons was 86.7% (95% CI, 69.5%, 100.0%).

A few enveloped capsids were observed within vesicles close to the membranes of the varicosities and growth cones. In these cases, examination at high magnification revealed that the vesicle membrane was continuous with the axonal membrane,

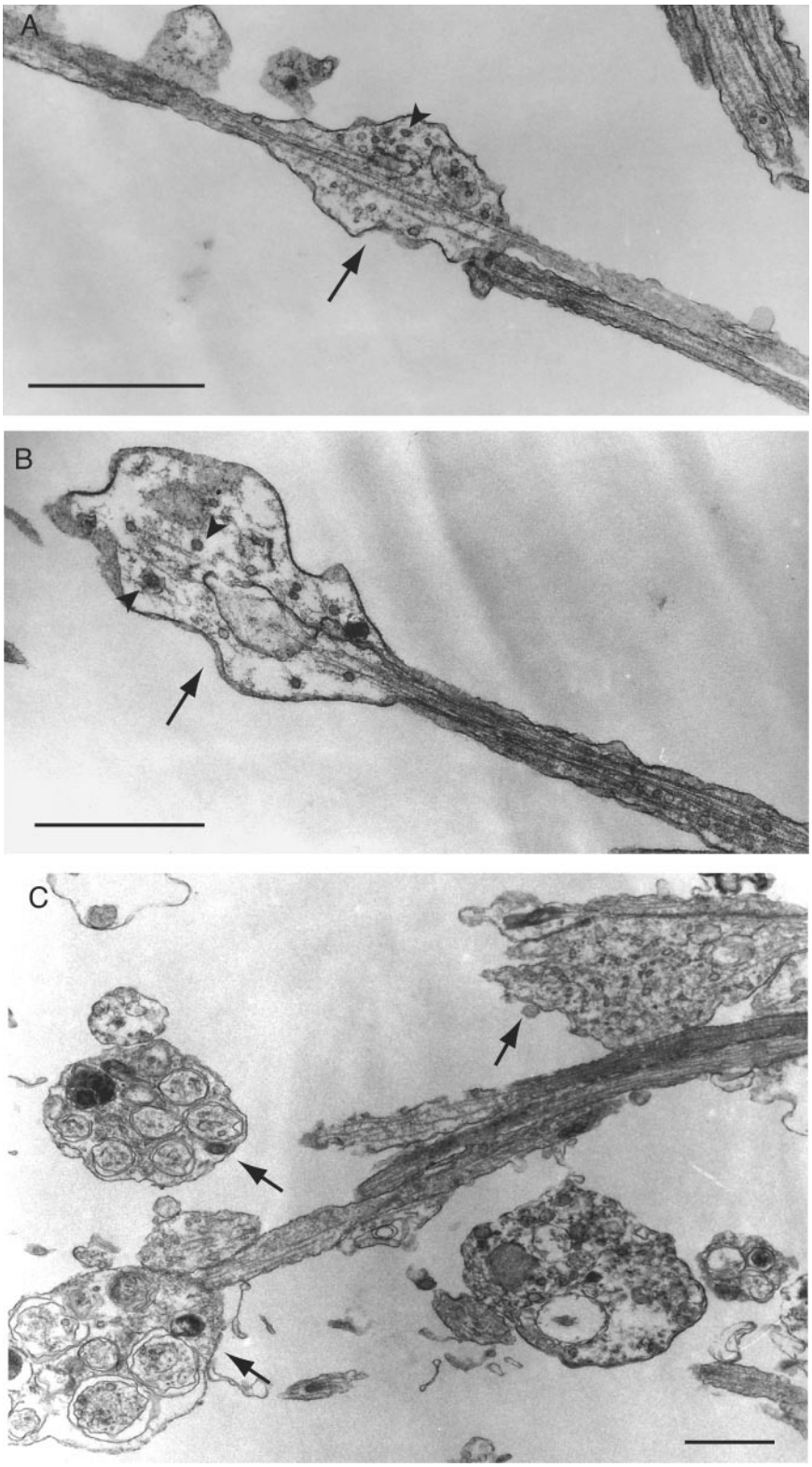

FIG. 5. Electron micrographs of mock-infected human DRG axons. Coverslips with explanted DRG cultures in situ were fixed and processed for TEM. Areas containing mid- and distal regions of axons were sectioned, collected on copper grids, and examined using a Philips CM120 BioTWIN transmission electron microscope at 100 kV. (A) An axonal varicosity (arrow) is an expanded region of the axon showing a disruption in microtubule bundles and contains numerous heterogeneous vesicles (arrowhead). Growth cones (B and C) (arrows) at the axon terminus are visible among the distal axons and have a central region containing a high concentration of heterogeneous vesicles (clear and dense core vesicles) (arrowheads) and a few microtubules, which are continuous with the axon that precedes the growth cone. Bars, 1 μm.

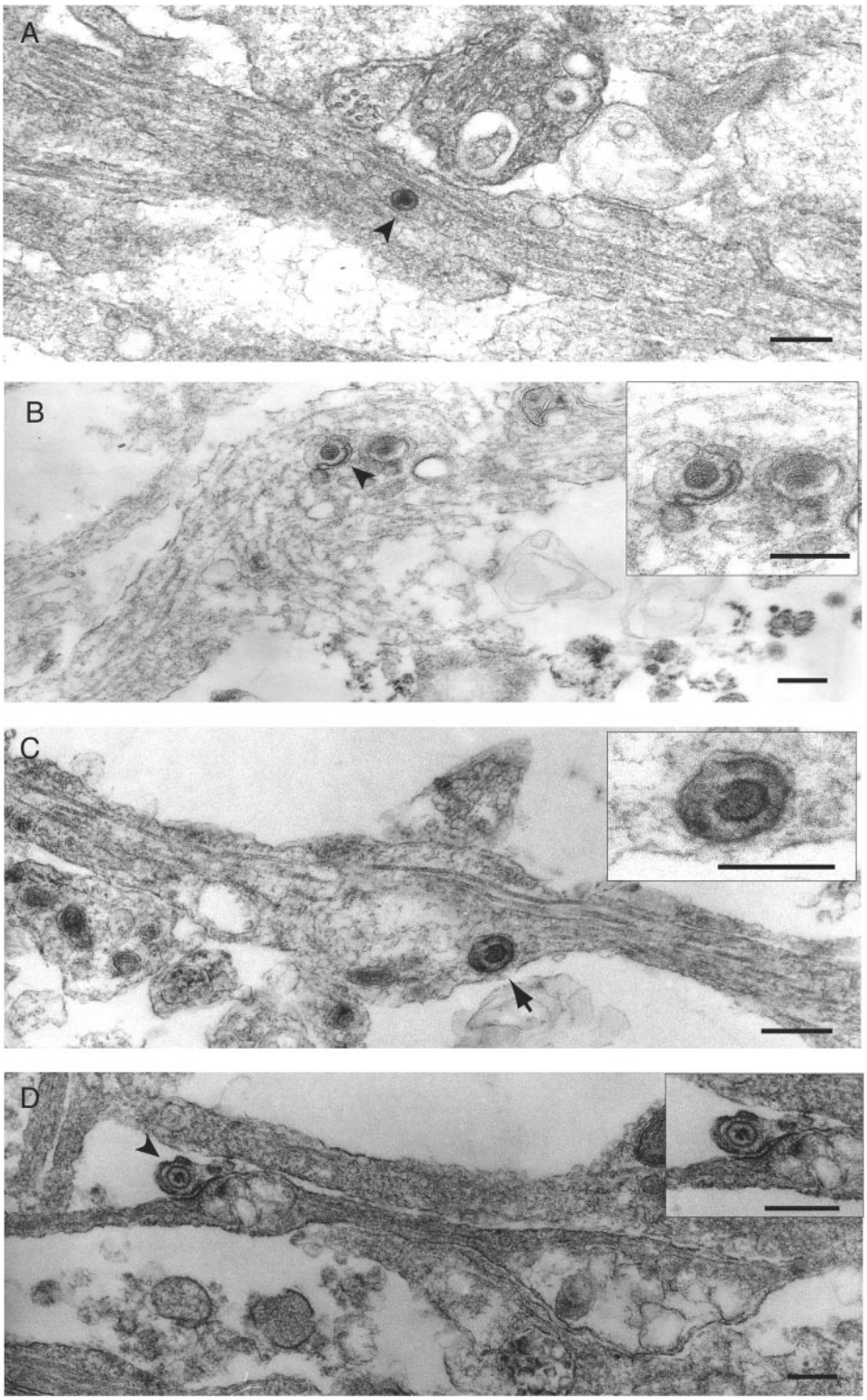

FIG. 6. Electron micrographs of HSV-1 particles in infected human DRG axons. Coverslips with explanted DRG cultures in situ were infected with the clinical isolate CW1 of HSV-1, fixed, and processed for TEM. Areas containing mid- and distal regions of axons were sectioned and examined. (A) Unenveloped capsid (arrowhead) in midaxon. (B) Partially enveloped capsid (arrowhead) in an expanded, vesicle-rich varicosity. The inset shows an enlargement of the viral particle, surrounded by a vesicular membrane. (C) Enveloped capsid in a vesicle (arrow) in a varicosity. The inset shows an enlargement of the enveloped capsid in a vesicle. (D) Extracellular viral particle (arrowhead) adjacent to a varicosity. The inset shows an enlargement of the viral particle in a thickened crescent-shaped invagination of the axonal plasma membrane. Bars, 200 nm.

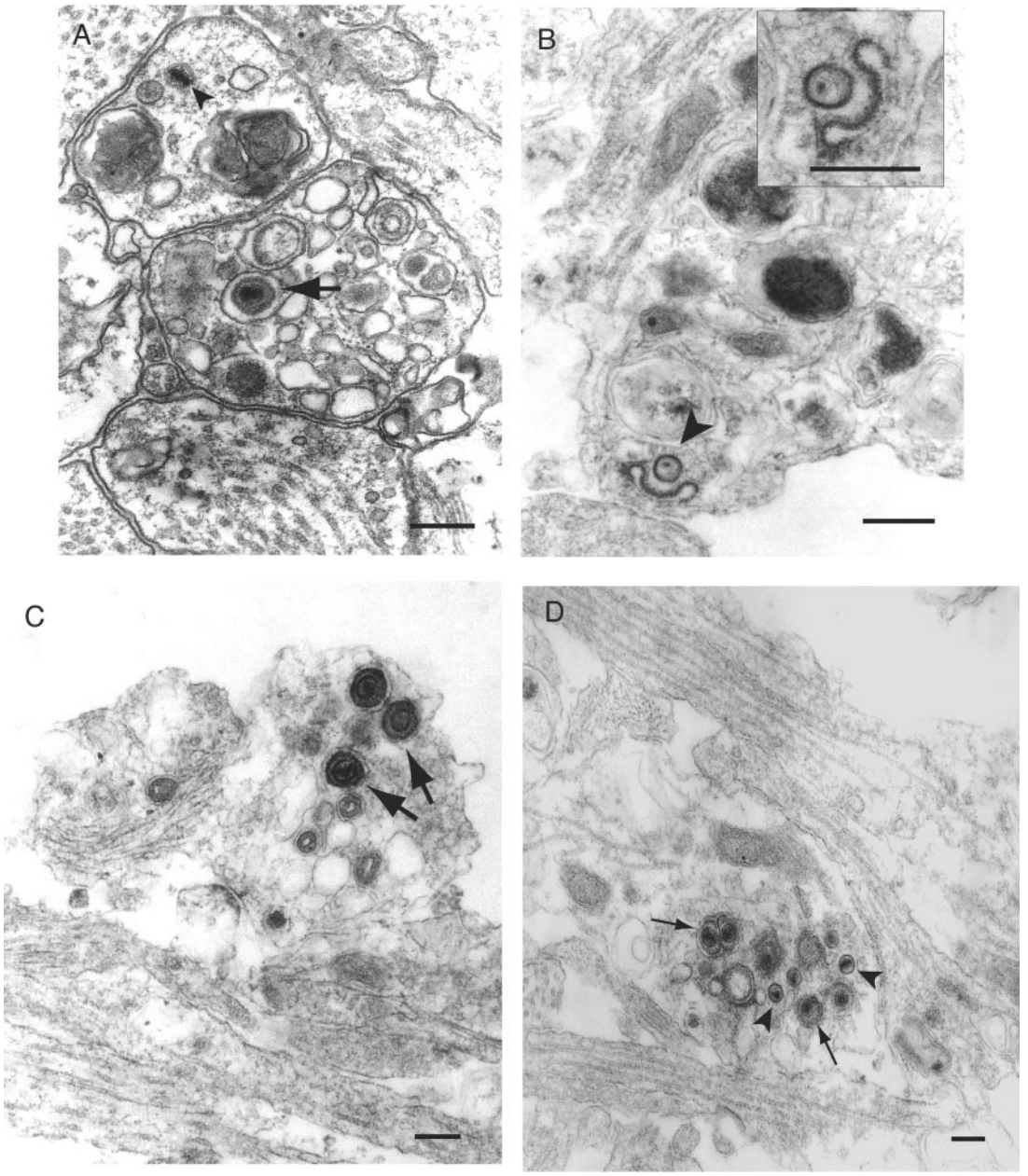

FIG. 7. Ultrastructural examination of viral particles in human DRG axons infected with HSV-1. Coverslips with explanted DRG cultures in situ were infected with the clinical isolate CW1 of HSV-1, fixed, and processed for TEM. Areas containing mid- and distal regions of axons were sectioned and examined. (A) Enveloped (arrow) and unenveloped (arrowhead) capsids in growth cones. (B) Partially enveloped capsid (arrowhead) in a growth cone. The inset shows an enlargement of the partially enveloped capsid. A dense, thickened membrane on the vesicle surrounding the viral particle is visible and probably represents tegument and envelope proteins. (C) Enveloped capsids in vesicles (arrows) in a growth cone. (D) Enveloped (arrows) and unenveloped (arrowheads) capsids in an axonal varicosity at an axonal bifurcation. Note the homogeneous size and morphology of unenveloped capsids, equivalent to those within the enveloped virions. Bars, 200 nm.

leaving an open channel to the extracellular space through which the virion might exit the axon (Fig. 9A), similar to those observed in relation to virions exiting from the neuronal cell body (31).

When cultures of human fetal DRG were infected with clinical isolate CW1 (10^5 PFU/0.5 ml/ganglion) and samples of culture medium were taken at 3, 6, 24, and 48 h p.i. for virus quantification on human fibroblasts, no infectious virus was detected in the supernatant until 48 h p.i. (median, 7×10^2 PFU/ml/ganglion). When examined by TEM, extracellular virions were observed adjacent to axonal varicosities, growth cones, and regions of axons adjacent to them. These increased markedly between 24 and 48 h p.i. (Table 2), consistent with the time of detection of extracellular infectious virus. Some of the extracellular virions appeared to sit within thickened crescent-shaped invaginations of the plasma membrane, similar

TABLE 2. Quantification of viral particles in mid- and distal axons

Capsid	No. at:	
	24 h p.i. (n = 1206)[a]	48 h p.i. (n = 768)[a]
Enveloped in axons	1	1
Unenveloped in axons	6	7
Enveloped in varicosities	24	10
Unenveloped in varicosities	3	7
Partially enveloped in varicosities	3	1
Enveloped in growth cones	25	11
Unenveloped in growth cones	6	3
Partially enveloped in growth cones	2	0
Extracellular	28[b]	150[b]

[a] The total numbers of axon processes and regions of axons examined were 1,206 at 24 h p.i. and 768 at 48 h p.i.
[b] $P < 0.001$ (Pearson chi-square test).

to virions exiting the cytoplasm of the cell bodies of neurons (Fig. 6D) (31, 36). Viruses adhering to axons during entry did not show this morphology.

Envelope glycoprotein D is transported in axonal vesicles, either independently or in association with tegument protein VP22. TIEM was used to look for the presence of envelope glycoproteins and tegument proteins in vesicles in growth cones. Human DRG cultures were infected with the HSV-1 clinical isolate CW1 and fixed at 24 h p.i. The DRG cultures were then processed for TIEM by freeze substitution. Dual immunogold labeling (5- and 10-nm gold particles) with antibodies to tegument protein VP22 and gD was performed. Some electron-dense vesicles in growth cones labeled either for VP22 or gD, while others labeled for both viral proteins

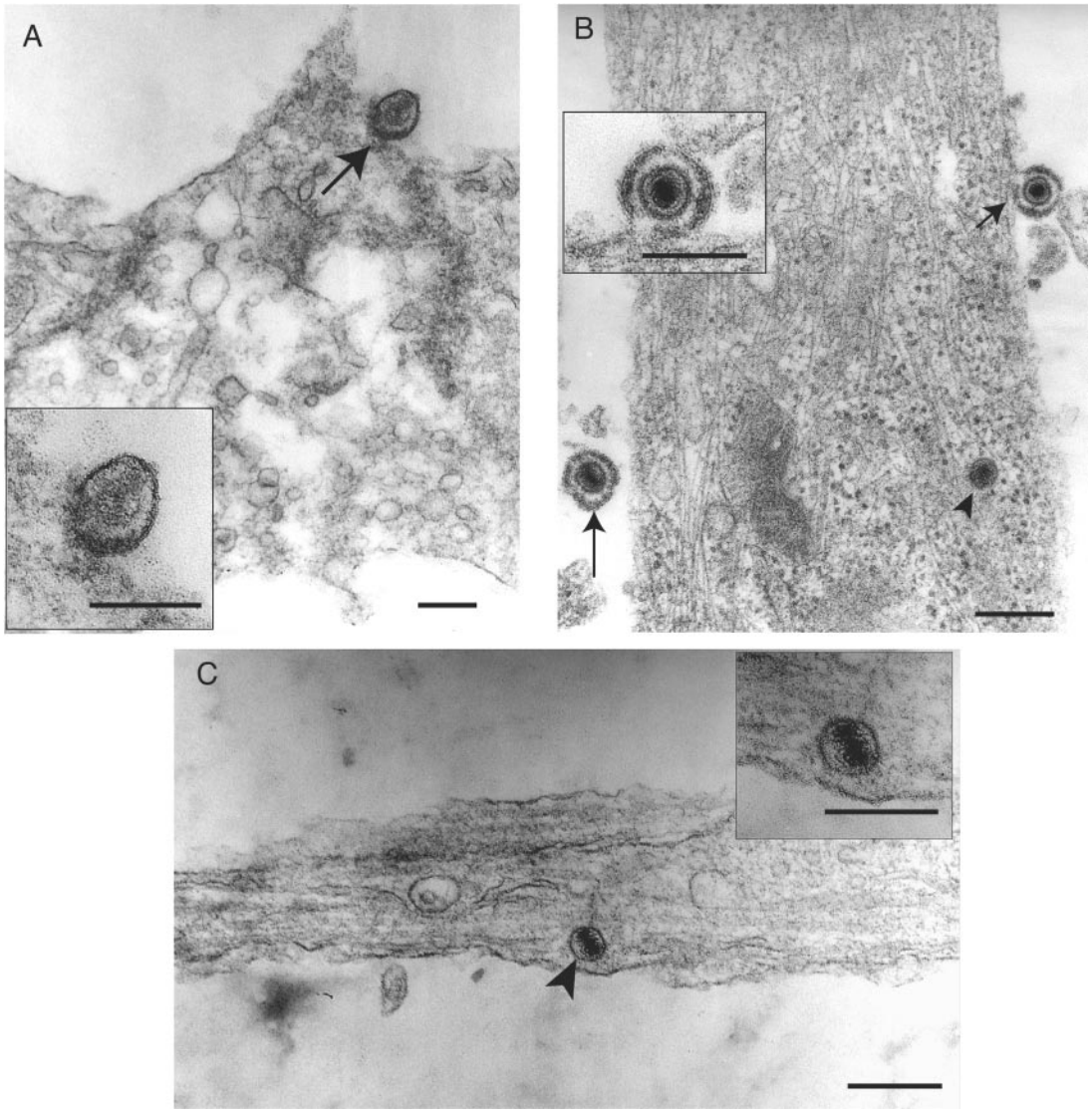

FIG. 8. Entry of HSV-1 into axons of explanted human DRG. Coverslips with explanted DRG cultures in situ were infected with the clinical isolate CW1 of HSV-1, fixed at 1.5 h p.i., and processed for electron microscopy. Areas containing mid- and distal regions of axons were sectioned and examined. (A) Enveloped virion (arrow) adherent to the plasma membrane of an axonal varicosity. The inset shows an enlargement of the viral particle. (B) Extracellular virion (arrow), viral particle (short arrow) bound to the axonal plasma membrane, and unenveloped capsid (arrowhead) inside the axon. The inset shows an enlargement of the adherent viral particle. (C) Unenveloped capsid (arrowhead) in an axon, subjacent to the axonal plasma membrane. The inset shows an enlargement of the unenveloped capsid. Bars, 200 nm.

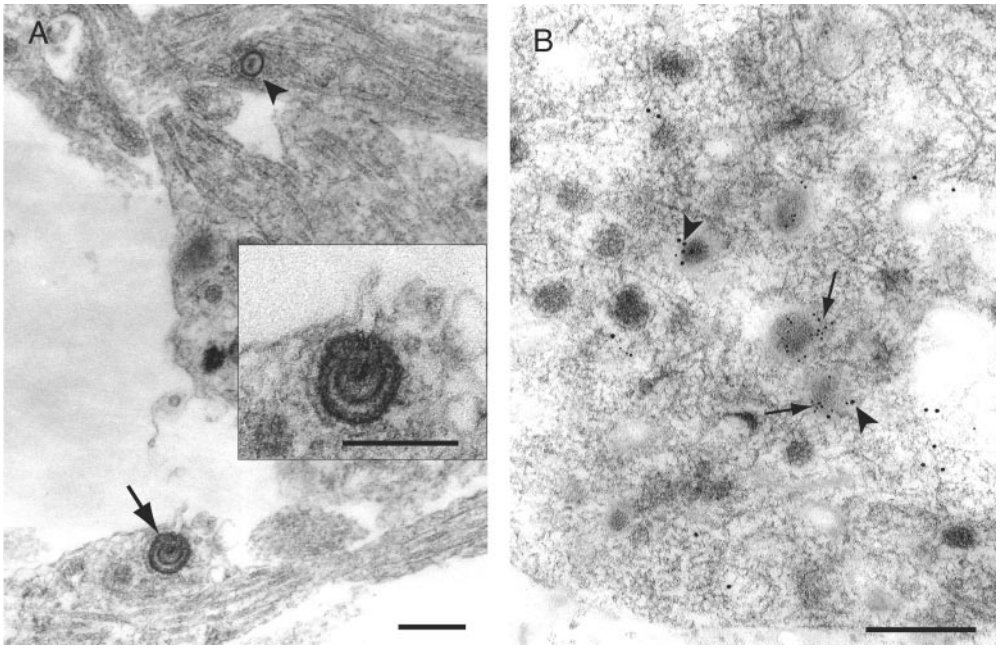

FIG. 9. Electron micrographs of HSV-1 particles in infected human DRG axons. Coverslips with explanted DRG cultures in situ were infected with the clinical isolate CW1 of HSV-1, fixed, and processed for electron microscopy. (A) Enveloped (arrow) and unenveloped (arrowhead) viral particles in varicosities. The membrane of the vesicle surrounding the enveloped capsid (inset) has fused with the axonal membrane, forming a pore to the surface, presumably allowing the virion to exit the axon. (B) Immunogold labeling of growth cones for tegument protein VP22 (5 nm) (arrows) and glycoprotein D (10 nm) (arrowheads). Label for VP22 (5 nm) is associated with vesicles either alone or together with gD (10 nm). Bars, 200 nm.

(Fig. 9B). Hence, tegument protein VP22 and glycoprotein D were found associated with vesicles in growth cones, either independently or in association with each other.

DISCUSSION

In this study, complementary approaches of immunofluorescence detection of HSV-1 proteins by confocal microscopy and electron microscopy were used to examine the process of HSV-1 transport and assembly in axons. The use of in situ fixation, processing, and longitudinal sectioning of axons allowed the localization of virions and cellular organelles to mid- and distal axons.

In human fetal DRG axons, colocalization of all three classes of HSV-1 components, capsid, tegument, and envelope proteins, was largely restricted to axonal varicosities and growth cones and was consistent with the presence of enveloped capsids in vesicles, which were observed in clusters at these sites by TEM. TIEM findings demonstrating the presence in growth cones of axonal vesicles associated with tegument (VP22) and envelope (gD) proteins, alone or together, were consistent with and also explained the confocal findings of free and colocalized proteins in these sites. Therefore, some tegument and envelope proteins may be transported separately or together, associated with axonal vesicles. These observations extend the findings for PRV in chick DRG neurons by real-time fluorescence (29) and are consistent with our previous TIEM studies of single tegument and envelope protein transport in axonal vesicles (23, 36). In concurrent studies of anterograde axonal HSV-1 transport in dissociated rat DRG neurons, we detected VP22 and gG proteins in the most distal regions of axons before VP5 and VP16 proteins, also consistent with free protein transport (unpublished data). Early availability of these proteins on vesicles in the distal axon could allow later assembly, as occurs in the *trans*-Golgi network. Colocalization of all three HSV-1 antigen classes was observed in the axon hillock and proximal axon but became attenuated rapidly in the midregions of the axon. These findings are consistent with recent reports of numerous enveloped PRV capsids in proximal SCG axons (5, 10), declining in numbers in the midaxon (5).

There could be two explanations for the partially enveloped capsids observed at 24 h p.i. in varicosities and growth cones: they may be assembling and exiting, or they may represent later reuptake of released virus by endocytosis. Entry of HSV-1 into cells by endocytosis rather than fusion with the cell membrane has now been reported by several laboratories and is cell type dependent (37, 40, 41). Following TEM examination of axons at 1 and 1.5 h p.i., we found adherent virions and submembranous unenveloped capsids along the length of axons, including varicosities and growth cones. However, no enveloped or partially enveloped capsids were seen at these times. This is consistent with recent reports by Nicola and coworkers and an earlier report by Lycke et al. that HSV-1 does not utilize endocytosis to enter neurons (30, 40, 41).

In addition, these partially enveloped capsids showed marked similarity to those observed enveloping in the Golgi complex in cultured cell lines and in the cell bodies of DRG neurons (20, 34, 36). Also, enveloped virions in crescent-shaped invaginations of the plasma membrane or in vesicles subjacent to the

membrane but connected to the surface by a pore were observed in both varicosities and growth cones, suggesting they were exiting at these sites (31, 34). There was a marked increase in the number of extracellular enveloped virions surrounding growth cones, varicosities, and regions of the axons adjacent to these sites from 24 to 48 h p.i., consistent with the appearance of extracellular infectious virus at 48 h p.i. Although there was a 10-fold increase in the number of extracellular virions from 24 to 48 h p.i., there was no corresponding increase in the numbers of partially enveloped capsids seen (Table 2).

Furthermore, there are two other quantitative arguments against the possibility that virus emerging from axons at 24 or 48 h p.i. might reinfect adjacent axons and contribute to the number of partially enveloped and unenveloped viral particles observed by TEM. First, virus only enters axons by anterograde transport between 19 and 24 h p.i., so the TEM observations at 24 h p.i. could not be explained by cross-infection. Secondly, the concentrations of virus, undetectable at 24 h p.i. and 7×10^2 PFU/ml at 48 h p.i., in supernatants are very low compared to the inoculum of 2×10^5 PFU/ml required for detection of virus entering axons at 1 and 1.5 h p.i. by TEM. Therefore, we estimate that more than 10,000 axons would need to be surveyed to detect one entering viral particle at 48 h p.i. (and more at 24 h p.i.). Thus, the most likely explanation of these partially enveloped virions in varicosities and growth cones is that they are enveloping prior to exit.

Superficially, these data showing mixtures of enveloped and unenveloped capsids present in focal collections in growth cones and varicosities appear inconsistent with our previous reports of only unenveloped capsids in cross sections of distal axons. This can be explained by the superior ability of the TEM technique used in this study to locate focal collections of enveloped virus in growth cones and varicosities and our focus on the mid- and distal regions of axons. In our studies, unenveloped capsids still predominated in the regions of axons between varicosities and growth cones. Rare enveloped capsids seen close to, but not within, varicosities and growth cones could either be the result of envelopment within the latter structures or represent transport of enveloped capsids from proximal axons. Our findings also conflict with a recent report showing only enveloped PRV capsids in proximal axons, except in the presence of brefeldin A (10), and with several of the reports shown in Table 1. However, the effects of brefeldin A on PRV in SCG neurons also appear to be markedly different from our report of HSV-1 in DRG neurons (35). Using twice the dose we used, del Rio and coworkers observed complete inhibition of axonal transport of PRV enveloped capsids, accumulation of unenveloped capsids in the cell body, and occasional unenveloped capsids in axons (10). Furthermore, we observed accumulation of enveloped HSV-1 capsids in the cell body and inhibition of axonal transport of envelope, but not capsid, proteins or capsids. How can these differences be explained? Although it seems unlikely that there will be completely different mechanisms of transport, assembly, and egress between PRV and HSV-1 in neuronal axons, substantial differences in other functions have been demonstrated between these distantly related alphaherpesviruses. The processes of anterograde transport of PRV in SCG neurons and HSV in DRG neurons seem similar, but they differ at least in degree. Ch'ng et al. reported that PRV capsid proteins entered mid-distal SCG axons by at least 14 h and that PRV can infect indicator PK15 cell lines via axons at 12 h (4, 5), whereas HSV-1 capsid proteins usually take approximately 24 h to enter axons (reference 35 and unpublished observations). Furthermore, we have never observed such large numbers of HSV-1 virions in (proximal) axons as reported for PRV in SCG neurons by del Rio et al. (10). Our previous observations of a delay in spread between cell body and axon suggest a filtering mechanism in the proximal axon or axon hillock (35, 36) that may be more restrictive for HSV-1 than for PRV, a hypothesis that is being explored. This hypothesis could be consistent with previous reports (Table 1) showing enveloped virions in axons where the region of the axon was defined as proximal and virions were often clustered in cisternae. Therefore, ongoing studies in our laboratory are directed at the proximal axon, using the new techniques. It will be interesting to determine whether the proximal axon contains a greater proportion of enveloped to unenveloped HSV-1 capsids, thus more closely resembling the cell body.

Recently, there have been technical advances in fluorescence and immunoelectron microscopic studies of anterograde axonal transport of alphaherpesviruses, but all continue to have problems, requiring the use of multiple techniques to complement their weaknesses. Thus, del Rio et al. (10) used combinations of dual-labeled capsid or tegument proteins and real-time fluorescence. This has the great advantage that colocalizing pairs of proteins can be observed during transport, but also the potential disadvantage that they may represent individual proteins traveling together rather than as components of virions. Further understanding of anterograde transport of PRV was shown by Luxton et al. (29). Using similar dual- labeled PRV virions and real-time fluorescence, they elegantly demonstrated the cotransport of UL36 (VP1/2) and UL37 tegument proteins with capsid during retrograde transport in DRG axons. However, during anterograde transport, five tegument proteins (UL36, UL37, VP13/14, VP16, and VP22) appeared to be cotransported with capsid VP26, although the cotransport of VP13/14 and VP22 was less consistent. In addition, these proteins were also capable of capsid-independent anterograde transport, similar to those described here and in our previous studies (23, 35, 36). The real-time fluorescence studies would be even more powerful if simultaneous labels for capsid, tegument, and envelope were available. In contrast, the advantages of serial fixation and simultaneous staining for capsid, tegument, and envelope proteins and colocalization by confocal microscopy are offset by the fact that these are not diffraction limited but measured within a discrete pixel area. Nevertheless, serial fixation allows direct detection of native protein, verifying that incorporation of label does not alter its transport properties.

TEM and TIEM are the only techniques that achieve the resolution required to identify capsids, but they are static techniques. They need to be used together with real-time fluorescence, or at least serial fixation, for appropriate interpretation. The electron microscopy techniques combined with longitudinal sections advance the field by allowing more accurate definition and sampling of different regions of the axon than were previously achieved with cross sections in the two-chamber model.

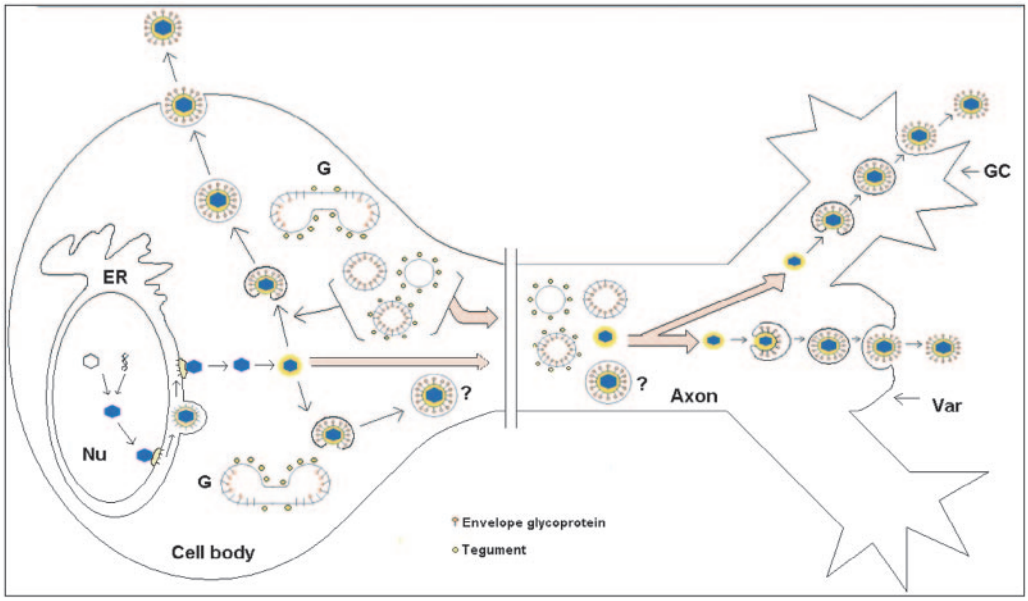

FIG. 10. Schematic diagram of the proposed model for assembly and egress of HSV-1 in varicosities and growth cones. Unenveloped capsids coated by inner tegument proteins are transported from the cell body into axons, accumulating in varicosities (Var) or growth cones (GC). At these sites, capsids invaginate vesicles, acquiring tegument and envelope proteins. These enveloped capsids, now contained within vesicles, exit locally via exocytosis. However, the possibility that enveloped HSV-1 capsids from the cell body also enter the mid- and distal regions of the axon and exit via the varicosities and growth cones cannot be excluded. ER, endoplasmic reticulum; G, Golgi; Nu, nucleus.

Taking into consideration some of the key studies in Table 1, especially recent reports (references 4, 5, and 10 and our own data), there appear to be two possible explanations for the apparently contradictory findings of enveloped versus unenveloped capsids in axons from different laboratories. One is that both enveloped and unenveloped HSV-1 and PRV capsids in both SCG and DRG neurons are transported into all regions of axons to different degrees for each system and exit via varicosities and growth cones. The other, our preferred option, is that enveloped HSV-1 capsids may exit from the DRG axon hillock and proximal axon by a mechanism similar to that in the cell body but that there is a filtering mechanism leading to selective transport of unenveloped capsids into the mid- and distal axons much greater than for PRV in SCG. These unenveloped capsids are coated by inner tegument proteins and are transported from the cell body into and along the axons via rapid kinesin/microtubule-mediated transport (11, 48). They then accumulate in varicosities or growth cones, where they assemble by invaginating vesicles transporting externally adherent tegument proteins and envelope proteins in the membrane and exit at these sites. The selective effects of gE, gI, and US9 in regulating PRV structural-protein transport into the distal rather than proximal axon could be consistent with such a hypothesis (4, 5). The separate, and perhaps faster, kinetics of transport of envelope glycoproteins and outer tegument proteins associated with axonal vesicles may prepare the distal axon for reenvelopment.

A minimal interpretation of our data is that there appear to be both enveloped and unenveloped capsids in varicosities and growth cones, with unenveloped capsids being significantly more frequent in the intervening regions between the varicosities. At least some and probably all of these unenveloped capsids are undergoing assembly and envelopment within the varicosities or growth cones and exiting by exocytosis. This is supported by the presence of tegument and envelope proteins in association with vesicles in the growth cones. Enveloped virions contained within vesicles probably exit locally via exocytosis by fusion of the vesicle membrane with the outer membrane of the varicosity or growth cone, releasing the virions into the extracellular fluid (Fig. 10). Recent data suggest that neurotransmitter-containing vesicles are transported distally from the central region of growth cones into their filopodia, probably along microtubules, to fuse with the plasma membrane (46). The possibility that HSV-1 has evolved to utilize this cellular function as a means of virus egress should be explored.

Furthermore, in cell lines and in the cell bodies of neurons, alphaherpesviruses acquire inner and outer tegument proteins sequentially at separate sites. The outer tegument proteins, including VP22, are probably acquired at the trans-Golgi network, followed by final envelopment (17, 34, 36). Envelopment of capsids by budding into vesicles bearing tegument and glycoprotein appears to be analogous in the cell body and the varicosities and growth cones. These vesicles could be derived from the Golgi, especially as some neuronal proteins, such as SCG10, traffic to all three sites (28, 38).

Therefore, how do these processes in cultured DRG neurons in vitro resemble those in nerves in vivo? Nerve growth factor (NGF) added in vitro induces frequent axonal branching, whereas in vivo axonal branching appears to be determined by a balance between inhibitory factors, such as semaphorins, secreted by mesenchymal cells, and stimulatory factors (NGF), secreted by epithelial cells (12, 18). Thus, the frequent axon branching seen in our neuronal cultures may resemble the plexus of unmyelinated fibers within the stratum granulosum (adjacent to NGF-secreting keratinocytes), which

would provide varicosities and growth cones as sites of viral egress with easy access to the epidermis.

ACKNOWLEDGMENTS

We thank Mary-Ann Lau for her help with Fig. 10 and Jacqueline Mills, Clinical Sciences, New Children's Hospital, Westmead, for assistance with confocal microscopy. We thank David McNab, MRC Virology Unit, Institute of Virology, United Kingdom, for excellent technical assistance with vUL37-GFP. We thank Karen Byth-Wilson, Westmead Millennium Institute and Westmead Hospital, for her assistance with statistical analysis and Claire Wolczak and Brenda Wilson, Westmead Millennium Institute, for clerical assistance. We also thank Carol Robinson, Levina Dear, and Gayle Versace-Avis, Electron Microscope Laboratory, ICPMR, Westmead Hospital, for assistance with electron microscopy and the members of the Animal Care Facility at Westmead Hospital for providing rat neonates.

This project was supported by project grant 253617 to A.L.C. from the National Health and Medical Research Council.

REFERENCES

1. **Bastmeyer, M., and D. M. O'Leary.** 1996. Dynamics of target recognition by interstitial axon branching along developing cortical axons. J. Neurosci. **16:**1450–1459.
2. **Bray, D.** 1973. Branching patterns of individual sympathetic neurons in culture. J. Cell Biol. **56:**702–712.
3. **Card, J. P., L. Rinaman, R. B. Lynn, B. H. Lee, R. P. Meade, R. R. Miselis, and L. W. Enquist.** 1993. Pseudorabies virus infection of the rat central nervous system: ultrastructural characterization of viral replication, transport and pathogenesis. J. Neurosci. **13:**2515–2539.
4. **Ch'ng, T. H., and L. W. Enquist.** 2005. Efficient axonal localization of alphaherpesvirus structural proteins in cultured sympathetic neurons requires viral glycoprotein E. J. Virol. **79:**8835–8846.
5. **Ch'ng, T. H., and L. W. Enquist.** 2005. Neuron-to-cell spread of pseudorabies virus in a compartmented neuronal culture system. J. Virol. **79:**10875–10889.
6. **Cohen, G. H., M. Ponce de Leon, H. Diggelmann, W. C. Lawrence, R. J. Vernon, and R. J. Eisenberg.** 1980. Structural analysis of the capsid polypeptides of herpes simplex virus type 1 and 2. J. Virol. **34:**521–531.
7. **Cook, M. L., and J. G. Stevens.** 1973. Pathogenesis of herpetic neuritis and ganglionitis in mice: evidence for intra-axonal transport of infection. Infect. Immun. **7:**272–288.
8. **Darlington, R. W., and L. H. Moss III.** 1968. Herpesvirus envelopment. J. Virol. **2:**48–55.
9. **deKort, E. J., A. A. Gribnau, H. T. van Aanholt, and R. Nieuwenhuys.** 1985. On the development of the pyramidal tract in the rat. The morphology of the growth zone. Anat. Embryol. **172:**195–204.
10. **del Rio, T., T. H. Ch'ng, E. A. Flood, S. P. Gross, and L. W. Enquist.** 2005. Heterogeneity of a fluorescent tegument component in single pseudorabies virus virions and envelope assemblies. J. Virol. **79:**3903–3919.
11. **Diefenbach, R. J., M. Miranda-Saksena, E. Diefenbach, D. J. Holland, R. A. Boadle, P. J. Armati, and A. L. Cunningham.** 2002. Herpes simplex virus tegument protein US11 interacts with conventional kinesin heavy chain. J. Virol. **76:**3282–3291.
12. **Dontchev, V. D., and P. C. Letourneau.** 2003. Growth cones integrate signalling from multiple guidance cues. J. Histochem. Cytochem. **51:**435–444.
13. **Douglas, M. W., R. J. Diefenbach, F. L. Homa, M. Miranda Saksena, F. J. Rixon, V. Vittone, K. Byth, and A. L. Cunningham.** 2004. Herpes simplex virus type 1 capsid protein VP26 interacts with dynein light chains RP3 andTcTex1 and plays a role in retrograde cellular transport. J. Biol. Chem. **279:**28522–28530.
14. **Elliott, G., G. Mouzakitis, and P. O'Hare.** 1995. VP16 interacts via its activation domain with VP22, a tegument protein of herpes simplex virus, and is relocated to a novel macromolecular assembly in co-expressing cells. J. Virol. **69:**7932–7941.
15. **Enquist, L. W., P. J. Husak, B. W. Banfield, and G. A. Smith.** 1998. Infection and spread of alphaherpesviruses in the nervous system. Adv. Virus. Res. **51:**237–347.
16. **Field, H. J., and T. J. Hill.** 1974. The pathogenesis of pseudorabies virus in mice following peripheral inoculation. J. Gen. Virol. **23:**145–157.
17. **Fuchs, W., B. G. Klupp, H. Granzow, C. Hengartner, A. Brack, A. Mundt, L. W. Enquist, and T. C. Mettenleiter.** 2002. Physical interactions between envelope glycoprotein E and M of pseudorabies virus and the major tegument protein UL49. J. Virol. **76:**8208–8217.
18. **Gallo, G., and P. C. Letourneau.** 1998. Localized sources of neurotrophins initiate axon collateral sprouting. J. Neurosci. **18:**5403–5414.
19. **Goldberg, J. L.** 2003. How does an axon grow? Genes Dev. **17:**941–958.
20. **Granzow, H., B. G. Klupp, W. Fuchs, J. Veits, M. Osterrieder, and T. C. Mettenleiter.** 2001. Egress of alphaherpesviruses: comparative ultrastructural study. J. Virol. **75:**3675–3684.
21. **Hill, T. J., H. J. Field, and A. P. C. Roome.** 1972. Intra-axonal localization of herpes simplex virus particles. J. Gen. Virol. **15:**253–255.
22. **Hill, T. J., and H. J. Field.** 1973. The interaction of herpes simplex virus with cultures of peripheral nervous tissue: an electron microscope study. J. Gen. Virol. **21:**123–133.
23. **Holland, D. J., M. Miranda-Saksena, R. A. Boadle, P. Armati, and A. L. Cunningham.** 1999. Anterograde transport of herpes simplex virus proteins in axons of peripheral human foetal neurons: an immunoelectron microscopy study. J. Virol. **73:**8503–8511.
24. **Johnson, D. C., and P. G. Spear.** 1982. Monensin inhibits the processing of herpes simplex virus glycoproteins, their transport to the cell surface, and the egress of virions from infected cells. J. Virol. **43:**1102–1112.
25. **Kristensson, K., B. Ghetti, and H. M. Wisniewski.** 1974. Study on the propagation of herpes simplex virus (type 2) into the brain after intraocular injection. Brain Res. **69:**189–201.
26. **LaVail, J. H., K. S. Topps, P. A. Giblin, and J. A. Garner.** 1997. Factors that contribute to the transneuronal spread of herpes simplex virus. J. Neurosci. Res. **49:**485–496.
27. **LaVail, J. H., A. N. Tauscher, J. W. Hicks, O. Harrabi, G. T. Melroe, and D. M. Knipe.** 2005. Genetic and molecular in vivo analysis of herpes simplex virus assembly in murine visual system neurons. J. Virol. **79:**11142–11150.
28. **Lutjens, R., M. Igarashi, V. Pellier, H. Blasey, G. Di Paolo, E. Ruchti, C. Pfulg, J. K. Staple, S. Catsicas, and G. Grenningloh.** 2000. Localization and targeting of SCG10 to the trans-Golgi apparatus and growth cone vesicles. Eur. J. Neurosci. **12:**2224–2234.
29. **Luxton, G. W., S. Haverlock, K. E. Coller, S. E. Antinone, A. Pincetic, and G. A. Smith.** 2005. Targeting of herpesvirus capsid transport in axons is coupled to association with a specific set of tegument proteins. Proc. Natl. Acad. Sci. USA **102:**5832–5837.
30. **Lycke, E., K. Kristensson, B. Svennerholm, A. Valhne, and R. Zeigler.** 1984. Uptake and transport of herpes simplex virus in neurites of rat dorsal root ganglia cells in culture. J. Gen. Virol. **65:**55–64.
31. **Lycke, E., B. Hamark, M. Johansson, A. Krotochwil, J. Lycke, and B. Svennerholm.** 1988. Herpes simplex virus infection of the human sensory neuron. An electron microscopy study. Arch. Virol. **101:**87–104.
32. **McLean, C., A. Buckmaster, D. Hancock, A. Buchan, A. Fuller, and A. Minson.** 1982. Monoclonal antibodies to three non-glycosylated antigens of herpes simplex virus type 2. J. Gen. Virol. **63:**297–305.
33. **Mettenleiter, T. C.** 2002. Herpesvirus assembly and egress. J. Virol. **76:**1537–1547.
34. **Mettenleiter, T. C.** 2004. Budding events in herpesvirus morphogenesis. Virus Res. **106:**167–180.
35. **Miranda-Saksena, M., P. J. Armati, R. A. Boadle, D. J. Holland, and A. L. Cunningham.** 2000. Anterograde transport of herpes simplex virus type 1 in cultured, dissociated human and rat dorsal root ganglion neurons. J. Virol. **74:**1827–1839.
36. **Miranda-Saksena, M., R. A. Boadle, P. J. Armati, and A. L. Cunningham.** 2002. In rat dorsal root ganglion neurons, herpes simplex virus type 1 tegument forms in the cytoplasm of the cell body. J. Virol. **76:**9934–9951.
37. **Milne, R. S. B., A. V. Nicola, J. C. Whitbeck, R. J. Eisenberg, and G. H. Cohen.** 2005. Glycoprotein D receptor-dependent, low-pH-independent endocytic entry of herpes simplex virus type 1. J. Virol. **79:**6655–6663.
38. **Morihara, T., A. Mizoguchi, M. Takahashi, S. Kozaki, T. Tsujihara, S. Kawano, M. Shirasu, T. Ohmukai, M. Kitada, K. Kimura, S. Okajima, K. Tamai, Y. Hirasawa, and C. Ide.** 1999. Distribution of synaptosomal-associated protein 25 in nerve growth cones and reduction of neurite outgrowth by botulinum neurotoxin A without altering growth cone morphology in dorsal root ganglion neurons and PC-12 cells. Neuroscience **91:**695–706.
39. **Nakata, T., S. Terada, and N. Hirokawa.** 1998. Visualization of the dynamics of synaptic vesicle and plasma membrane proteins in living axons. J. Cell Biol. **140:**659–674.
40. **Nicola, A. V., A. M. McEnvoy, and S. E. Straus.** 2003. Roles for endocytosis and low pH in herpes simplex virus entry into HeLa and Chinese hamster ovary cells. J. Virol. **77:**5324–5332.
41. **Nicola, A. V., J. Hou, E. O. Major, and S. E. Straus.** 2005. Herpes simplex virus type 1 enters human epidermal keratinocytes, but not neurons, via a pH-dependent endocytic pathway. J. Virol. **79:**7609–7616.
42. **Ohara, P. T., M. S. Chin, and J. H. LaVail.** 2000. The spread of herpes simplex virus type 1 from trigeminal neurons to the murine cornea: an immunoelectron microscopy study. J. Virol. **74:**4476–4486.
43. **Ohara, P. T., A. N. Tauscher, and J. H. LaVail.** 2001. Two paths for the dissemination of herpes simplex virus from infected trigeminal ganglia to the murine cornea. Brain Res. **899:**260–263.
44. **Penfold, M. E. T., P. A. Armati, and A. L. Cunningham.** 1994. Axonal transport of herpes simplex virions to epidermal cells: evidence for a specialized mode of virus transport and assembly. Proc. Natl. Acad. Sci. USA **91:**6529–6533.
45. **Roizman, B., and A. E. Sears.** 1996. Herpes simplex viruses and their replication, p. 2231–2296. *In* B. N. Fields, D. M. Knipe, and P. M. Howley (ed.), Fields virology, 3rd ed. Raven Press, Philadelphia, Pa.

46. **Sabo, S. L., and A. K. McAllister.** 2003. Mobility and cycling of synaptic protein-containing vesicles in axonal growth cone filopodia. Nat. Neurosci. **12:**1264–1269.
47. **Skepper, J. N., A. Whiteley, H. Browne, and A. Minson.** 2001. Herpes simplex virus nucleocapsids mature to progeny virions by an envelopment→ deenvelopment→reenvelopment pathway. J. Virol. **75:**5697–5702.
48. **Smith, G. A., L. Pomeranz, S. P. Gross, and L. W. Enquist.** 2004. Local modulation of plus-end transport targets herpesvirus entry and egress in sensory neurons. Proc. Natl. Acad. Sci. USA **101:**16034–16039.
49. **Stackpole, C. W.** 1969. Herpes-type virus of the frog renal adenocarcinoma: virus development in tumor transplants maintained at low temperature. J. Virol. **4:**75–93.
50. **Tennyson, V. M.** 1970. The fine structure of the axon and growth cone of the dorsal root neuroblast of the rabbit embryo. J. Cell Biol. **44:**62–79.
51. **vanGerderen, I. L., R. Brandimarti, M. R. Torisi, G. Campadelli-Fiume, and G. vanMeer.** 1994. The phospholipid composition of extracellular herpes simplex virions differs from that of host cell nuclei. Virology **220:**831–836.
52. **Wald, A., L. Corey, R. Cone, A. Hobson, G. Davis, and J. Zeh.** 1997. Frequent genital herpes simplex virus 2 shedding in immunocompetent women. Effect of acyclovir treatment. J. Clin. Investig. **99:**1092–1097.
53. **Yamamoto, T., S. Otani, and H. Shiraki.** 1973. Ultrastructure of herpes simplex infection of the nervous system of mice. Acta Neuropathol. **26:**285–299.
54. **Yuan, A., R. G. Mills, J. R. Bamburg, and J. J. Bray.** 1997. Axonal transport and distribution of cyclophilin A in chicken neurones. Brain Res. **771:**203–212.